ISSN: 2995-3286

Research Article

International Journal of Media and Networks

The Role of Greenhouse Gases, Aerosols, and Deforestation in Climate Change: a Multidisciplinary Assessment of the Interaction Mechanisms Between Human Activity and the Environment

Abderrazak Arif*

National Institute of Meteorology B.P. 156, 2035 Tunis-Carthage, Tunisia.

***Corresponding Author**
Abderrazak Arif, National Institute of Meteorology B.P. 156, 2035 Tunis-Carthage, Tunisia.

Submitted: 2024, Jan 30 **Accepted:** 2024, Feb 20 **Published:** 2024, Feb 29

Citation: Arif, A. (2024). The Role of Greenhouse Gases, Aerosols, and Deforestation in Climate Change: a Multidisciplinary Assessment of the Interaction Mechanisms Between Human Activity and the Environment. *Int J Med Net, 2*(2), 01-14.

Abstract

Climate change can be caused by various anthropogenic or natural factors that influence atmospheric changes. The direct link between human activity and the environment is represented by the interaction mechanisms between anthropogenic factors such as urbanization, deforestation, hydrological changes, greenhouse gases and aerosols. These interaction mechanisms are assessed by the current state of knowledge in the climate change field.

One of these mechanisms is related to greenhouse gases (GHGs), which increase surface level heating and lowers atmospheric temperature in the long term by increasing atmospheric GHG concentration. This heating reduces air density parcel and increases total evaporation to transfer excess heat from surface (latent heat) to atmosphere.

Another mechanism is related to anthropogenic aerosols, which have direct and indirect effects on climate change with variable direct radiative forcing depending on the nature, density and composition of the aerosol particles. Anthropogenic sulphate is the main element that influences atmospheric conditions through its direct and indirect effects, which delay global warming by increasing the albedo and the lifetime of clouds formed by water droplets.

A third mechanism is related to deforestation, which affects the environment according to the results of climate models based on deforestation scenarios. Deforestation alters the heat exchange between the oceans (relatively warm) and the atmosphere (relatively cold), generating a sensible heat flux (warming) that influences neighbouring regions. Deforestation also lowers surface temperature by changing coniferous vegetation to tundra and desert, causing a cooling of up to -4°C in North America and -6°C in Siberia. In Europe, deforestation scenarios show a decrease in surface temperature of -2°C to -3°C in spring and -1°C in summer in northern mid-latitudes, mainly due to the delayed melting of spring snow.

Keywords: Climate, Aerosols, GHGs, Deforestation, Human Activity, Heating, Cooling, Climate Change.

1. Introduction

The climate is explained mainly by the interactions between many components of the Earth system. The main drivers of the Earth's climate system are the atmosphere and the oceans, were exchange large amounts of energy through ocean currents, winds, evaporation and precipitation. The climate of a given location on the globe is usually stable over a century scale, but it can change significantly over geological time due to natural or anthropogenic factors.

The climate of a region can be characterized by its mean temperature and precipitation, and their seasonal variations. These variables depend mainly with latitude, longitude, altitude and proximity to water bodies. Other factors that can influence climate are solar radiation, the tilt and rotation of the Earth. Thus, solar radiation was affected by land surface, sea surface, ice cover, vegetation, wildlife and human activities.

We will study in this article human activities effects on the climate system through three main mechanisms: the greenhouse gases (GHG), the aerosols and the deforestation. We will use the climate models results to simulate the mechanisms effects on atmospheric changes. We will focus on the Mediterranean region, which covers a large area of Europe, Western Asia, the eastern Atlantic Ocean and North Africa (20 to 55 degrees latitude and - 20 to 30 degrees longitude). We will compare

climate data from two periods: the pre- industrial period (1948-1976) and the modern period (1977-2021). We will analyze the variability of temperature and precipitation between these two periods through their anomalies and explain the physical causes.

Greenhouse Gases (GHG)

GHGs are gases that absorb a quantity of atmospheric radiation which contribute to climate change. The carbon dioxide (CO2), methane (CH4), nitrous oxide (N2O), hydrofluorocarbons (HFCs) and sulphur hexafluoride (SF6) represents the main anthropogenic GHGs. These GHGs are emitted following human activities where the use of fossil fuels, agriculture, land use change, industry and waste management are implied.. According to the Ministère de la Transition Écologique de la France (2021), GHG emissions related to human activities represented the equivalent of 55.3 billion tonnes of CO2 in 2018, with CO2 accounting for 75% of these emissions.

The global CO2 emission increased by 1.9% in 2018, reaching a level that was more than 65% higher than in 1990. However, there were significant differences among countries in terms of their emissions levels and trends. China was the largest emitter of CO2 in 2018, with 30% of the global share, followed by the United States with 14% and the European Union with 8%. On average, each person in the world emitted 5.0 tonnes of CO2 per year in 2018, which was 16% more than in 1990.

According to Easterling et al. (1997), IPCC (2001a) and Sha Zhou et al. (2023), the increase of the atmospheric GHG concentration enhances the natural greenhouse effect, which is the process by which the Earth's surface and lower atmosphere are warmed by the absorption and re-emission of infrared radiation by GHGs. This may cause an increase in the global surface temperature mean, which can affect various aspects of the climate system, such as precipitation patterns, sea level rise, extreme weather events, ice melt, ocean acidification and loss of biodiversity [2-4]. The Intergovernmental Panel on Climate Change (IPCC) estimates that the global mean temperature has increased by about 1.1°C since the pre-industrial period (1850-1900), and projects that it will increase by 1.5°C to 4.5°C by 2100 depending on the future GHG emission scenarios.

According to the IPCC (2000), about 270 giga tonnes of carbon were released into the atmosphere from 1850 to 1998 due to fossil fuel use and cement production. The CO2 concentration increased from 278 ppmv in the pre-industrial period to 410 ppmv in 2019 [5]. This increase has accelerated since the mid-1960s, reaching an annual mean increase of 2.6 ppmv from 2018 to 2019.

Since the pre-industrial era (1750), anthropogenic gas emissions have had a significant impact on the greenhouse effect, as they absorb infrared radiation emitted by the Earth's surface and re-emit it back to the atmosphere. The absorption rate of this terrestrial energy depends on the atmospheric GHG concentration and the layer thickness that absorbs it. Among the GHGs, water vapor (H2O) plays a predominant role and contributes to 62.5% of this effect, but its concentration is variable in the atmosphere with time and space. Other gases such as CO2, CH4, N2O, O3 and CFCs have a considerable influence on the greenhouse effect in the atmosphere, as they have increased considerably over the past century due to human activities.

	GWP, Global Warming Potential (eq CO_2)	
	over a period of 20 years	over a period of 100 years
CO_2 (carbon dioxide)	1	1
CH_4 (methane)	84	28
N_2O (nitrous oxide)	264	265
CF_4 (carbon tetrafluoride)	4880	6630
HFC-152a (1,1-difluoroethane)	506	138

Table 1: Conventional values of greenhouse gases in "CO2 equivalent", according to the 5th report of the IPCC (2014).

Table 1 shows the conventional values of GHGs in CO2 equivalent in the atmosphere [6]. CO2 is the dominant gas, accounting for 79% of the greenhouse effect, followed by CH4 with 14% and N2O with 5%. The IPCC (1996) showed that the concentrations of CO2, CH4 and N2O increased respectively by 30%, 45% and 15% between 1750 and 1992 due to human activities. The CO2 concentration increased from 278 ppmv in the pre-industrial period to 410 ppmv in 2019 [5]. The CO2 emissions from 1850 to 2019 were 2400±240 GtCO2, of which nearly 58% occurred between 1850 and 1989, and nearly 42% occurred between 1990 and 2019. The atmospheric CO2 concentration in 2019 was higher than at any time for at least 2 million years [7].

The increase in atmospheric GHG concentration enhances the natural greenhouse effect, which leads to a rise in global mean temperature. This affects various aspects of the climate system, such as precipitation patterns, sea level rise, extreme weather events, ice melting, ocean acidification and biodiversity loss.

Forests have an important regulator in of the atmospheric GHG concentration, as they absorb a significant amount of CO2 from the atmosphere through photosynthesis. Thus, forests act as GHG sinks, storing carbon in their biomass [7-12]. However, forests can also become sources of GHGs when they release carbon into the atmosphere due to forest fires or land conversion

to agriculture or urban areas. Therefore, deforestation can causes the GHG emissions and change the climate [13].

1.2 Physical Effects

The Earth's climate system is influenced by the energy from space, mainly from the sun. The sun emits radiation with wavelengths ranging from 0.2 μm to about 4 μm (Figure 1), including ultraviolet (shortest wavelength), visible (between 0.40 μm and 0.80 μm) and infrared (longest wavelength). The visible radiation represents almost half of the total energy that reaches the atmosphere. Some of this radiation is absorbed by atmospheric components such as clouds, CO2 (55%), CH4 (15%) and N2O (6%), while some is reflected back to space by the Earth's surface [14].

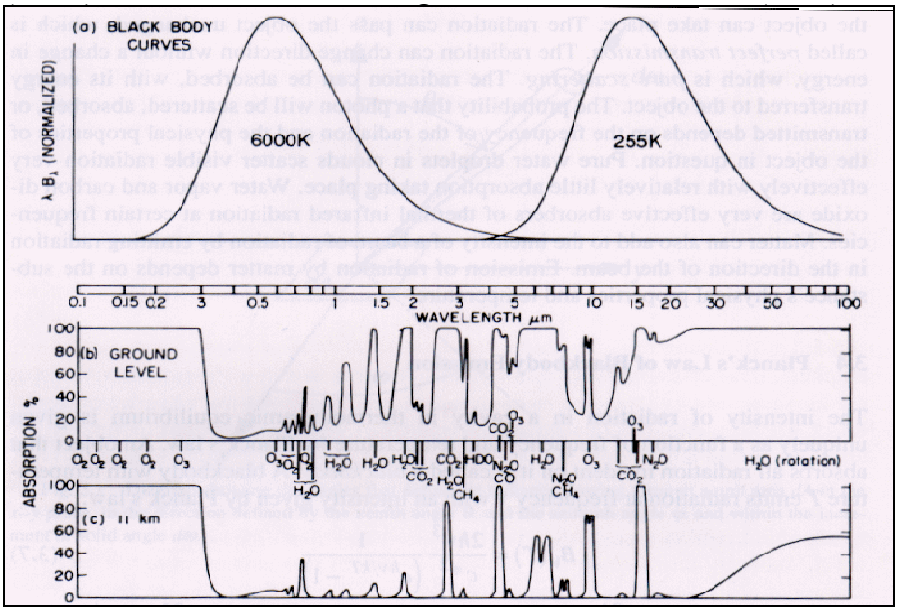

Figure 1: Spectral emission of a black body for the sun (6000K) and the earth (255K) as a function of wavelength, taken from Hartmann (1994).

In reality, not all of the visible energy from the sun is absorbed by the earth-atmosphere system. About 30% of this energy is reflected back to space by the surface, clouds, and aerosols. The remaining 70% is the net flow of energy that heats up the planet (the global

mean value of this heating is 240 W m-2). To maintain thermal equilibrium, the earth- atmosphere system also emits infrared radiation to space. This emission originates from either the earth's surface or from gases and clouds in the atmosphere.

Atmospheric gases and clouds play a major role in the thermal balance of the earth- atmosphere system. The natural greenhouse effect adds more than 2.5 W m-2 (nearly 1% of the planetary energy flow) to the system, with the largest contribution coming from CO2 [6,7,15-17]. Nearly half of this thermal contribution comes from other GHGs such as methane (CH_4), nitrous oxide (N_2O), CFCs and tropospheric ozone (O_3). However, an increase of these atmospheric gases concentration (due to anthropogenic GHGs) may lead to a change in the global temperature that could cause an increase in the earth-atmosphere heating.

1.2.1 Data Analysis

The data analysis for the northern hemisphere indicates that, during the 20th century, the surface temperature increase was the most pronounced in the past 1000 years [3,7]. The main anthropogenic GHGs [carbon dioxide (CO2), methane (CH4), nitrous oxide (N2O) and tropospheric ozone (O3)] have experienced record increases since 1990 due mainly to the use of fossil fuels, agriculture and land use [18]. CO2 is the most important of these GHGs since its concentration in the atmosphere has risen considerably in recent decades [3,6,7,17]. To understand how these GHGs interact with the atmosphere, we will rely on the climate results from the atmospheric General Model Circulation (GMC).

Climate models are generally used to predict future climate with GHGs forcing and other factors that can influence atmospheric processes, such as aerosols, deforestation or

urbanization. The IPCC (2023) reported that GHG forcing resulted in a doubling of CO2 concentration by 2100 for the high and very high GHG emissions scenarios, and by 2050 for the intermediate GHG emission scenario [7]. The intermediate GHG emission scenario has CO2 emissions remaining around current levels through mid-century. The very low and low GHG emissions scenarios have CO2 emissions declining to net zero around 2050 and 2070, respectively, followed by varying levels of net negative CO2 emissions.

The climate system has experienced a remarkable increase in the global radiative forcing as a result of GHG effect during the last decade [7,17,20]. This forcing is estimated from indicators related to anthropogenic and natural influences on the atmosphere (Figure 2). The IPCC (2001a) reported an increase in global radiative forcing of 1.46 Wm-2 due to the

CO2 concentration increase, an increase of 0.48 Wm-2 due to the CH4 concentration increase, and an increase of 0.15 Wm-2 due to the N2O concentration increase in the atmosphere for the year 2000, giving a total positive radiative forcing of 2.43 Wm-2. On the other hand, a negative radiative forcing of -0.15 Wm-2 was estimated due to the reduction of stratospheric ozone (O3). Thus, it was estimated that tropospheric ozone increased by 36% since 1750. This increase in global radiative forcing corresponded to 0.35 Wm-2 (Figure 2), varying considerably from one region to another [3].

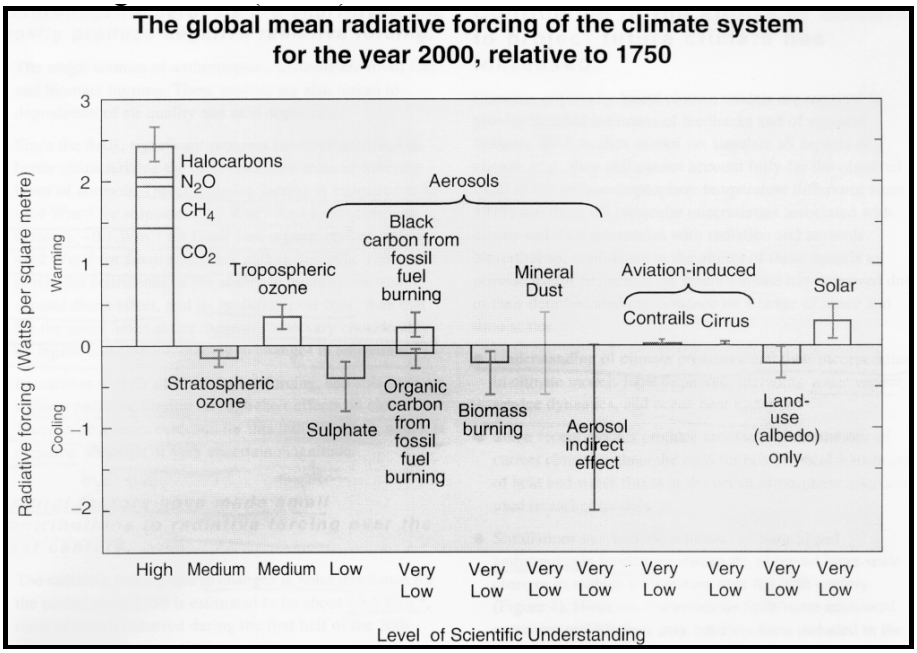

Figure 2: Different global radiative forcings by external climatic factors, according to IPCC (2001a).

1.3 Deforestation

The forest plays an important role in the climate balance at global scale. Vegetation changes can affect climatic conditions by altering the carbon cycle, the water cycle, and the energy balance [21,22]. Vegetation growth enhances heat transfer and increases the height of the Earth's boundary layer, the

lowest part of the atmosphere that is highly sensitive to surface radiation. This increase in turn affects cloudiness and surface radiation. On the contrary, the degradation of vegetation increases the surface albedo, which reduces the amount of solar radiation absorbed by the ground, which could cool the surface. In addition, total evaporation would decrease considerably following the removal of vegetation [23,24]. These two parameters (ground albedo and evaporation) can significantly influence the atmosphere and climate.

The logging of forest wood poses a challenge related to human activity that could alter the climate. In Canada, approximately one million hectares of forest are harvested annually [10]. The construction of dams could also greatly affect the water balance in these regions. Large hydroelectric dams, for example, have led to the degradation of forests and wildlife habitats as well as the significant reduction of water in lakes and rivers for electricity generation (GCSI and Environnement Canada, 1997 and 1999). Fog formation, temperature variation due to water heat capacity, humidity variation, precipitation, soil erosion and evapotranspiration are among the main factors that could be modified by the effect of hydroelectric reservoirs.

Moreover, Potter et al. (1981) showed that increasing soil albedo cools the surface slightly [25]. Price and Rind (1994) explained that a change in vegetation increases the ground albedo by causing a reduction in the amount of solar radiation absorbed by the ground surface, which can then cool the surface [26]. Crowley and Baum (1997) explained that a large decrease in surface temperature, accompanied by an increase in albedo, is due to changes in vegetation [27]. Douville and Royer (1997) showed that the effect of deforestation would cause surface cooling due mainly to the delay in snow melting in spring [28]. Wyputta and McAvaney (2001) mentioned that vegetation influences climate mainly through its effects on surface albedo, evaporation, transpiration and ground roughness [21]. On the other hand, Xue et al. (1990) showed that increasing ground albedo is followed by surface warming [29]. Following the soil albedo change, the surface temperature variability depends on the increase and/or decrease in soil moisture as the vegetation cover changes [30]. Data observed in China and Brazil has shown that the increase in surface temperature and the decrease in precipitation are the results of a decrease in tropical forest cover, which increases the surface albedo mentioned that the surface albedo has a large role in determining the surface energy balance and that the radiative forcing induced by the albedo has a significant impact on climate and environment [31-33].

1.3.1 Physical Effects

The radiation balance in the atmosphere plays an essential role in the surface thermal balance that is involved in several physical and dynamic processes. The solar radiation absorption

and the radiation emission by the earth's surface are physical processes that can modify the radiative balance. Thus, the heat exchange associated with water phase changes, such as the latent heat released during the condensation of water vapor in clouds, influences the atmospheric heat balance and causes instability in the convective air parcels [34,35].

The net radiative energy at the surface is the sum of the solar and terrestrial fluxes,

defined by

$$R_s = S^{\downarrow}(0) - S^{\uparrow}(0) + F^{\downarrow}(0) - F^{\uparrow}(0) \quad (2.1)$$

Where S↓(0) and S↑(0) represent, respectively, the downward and upward fluxes of solar radiation at the surface, and F↓(0) and F↑(0) represent, respectively, the downward and upward fluxes of terrestrial radiation (longwave radiation) at the surface.

The albedo is the representative parameter that can influence the radiative characteristics of the surface. This parameter affects the net downward solar energy flux; it is defined as the fraction of upward solar flux that is reflected by the surface.

$$\alpha_s = \frac{S^{\uparrow}(0)}{S^{\downarrow}(0)} \quad (2.2)$$

The surface albedo varies widely with the surface and the atmospheric conditions, ranging from 5% (minimum) for the oceans in low wind speeds, up to 90% for fresh snow. Surface albedo also varies with solar zenith angle, wind speed, and the chemical composition of water in oceans, seas, and lakes. The presence of a cloud greatly changes the surface albedo, depending mainly on its optical thickness [36]. In northern regions, deforestation increases the surface albedo in winter, spring and early summer due to the snow accumulation in winter and the delayed melting in spring. This variability could directly influence the physical parameters of the surface and the atmosphere.

1.3.2 Data Analysis

Since the 1980s, GCMs have been used to study climate for various scenarios. The CO_2 doubling example has been used to examine the possible implications of the GHG effect on climate [37-41]. Other experiments have analyzed the potential effect of deforestation in northern regions

[15,42,43,28]. Otterman et al (1984) suggested a -1.9°C decrease in surface air temperature in a treeless forest in the northern hemisphere. Harvey (1988) confirmed that the replacement of ice cover by vegetation leads to a significant warming of the earth's surface [42]. Thomas and Rowntree (1992) showed that the absence of forest in the UK Meteorological Office (UKMO) Global Climate Model (GCM) would cause a - 8°C decrease in surface temperature in spring and delay snowmelt during this season. Chatila and Le Treut (1994) from the Laboratoire de Météorologie Dynamique (LMD) found a decrease in surface temperature following forest removal in the GCM [44].

The results of the global climate model ARPEGE (Action Recherche Petite Échelle Grande Échelle), developed by Météo-France and the European Center for Medium-Range Numerical Prediction (ECMWF), are presented in the form of two simulations [45]. The first simulation shows the results for a current climate scenario (CTR control experiment for four years). The second simulation explores a scenario of deforestation in the boreal region during the same four-year period (DEF experiment). All northern forests above latitude 45°N have been replaced by grasslands. This change will affect the climatic conditions in these regions.

The results from the ARPEGE model showed seasonal variation in the mean zonal anomalies of snow depth, clear-sky surface albedo, and surface air temperature over the continental northern hemisphere (Figure 3). In spring at mid-latitudes, the deforestation simulation in ARPEGE delayed snowmelt. The maximum of the zonal average snow depth anomaly exceeded 10 cm in May at 60°N latitude. The snow melted completely by the end of August at the 60°N latitude and by the end of June at the 45°N latitude in these regions (Figure 3). This delay in snowmelt postponed the warm summer season. Thus, the maximum increase of the albedo occurred in spring when it rose by 10% in a deforestation scenario during the cold period (February-June: Figure 3). This cooling is clearly visible in Figure 3 where the mid-latitude surface temperature anomaly was between -2°C and -3°C in spring. This cooling was relatively lower during the summer season when its anomaly decreased due to the delayed snowmelt in spring.

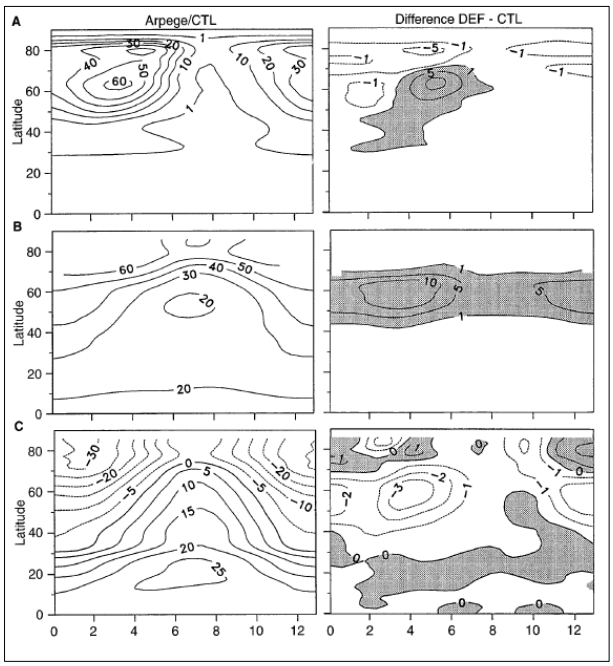

Figure 3: Seasonal cycle of zonal mean anomalies of A) snow depth (cm), B) clear-sky ground albedo (%) and C) surface air temperature (°C) in continental northern hemisphere. The abscissa axis describes the months of the year, according to Douville and Royer (1997).

Douville and Royer (1997) explained the cooling from the surface energy balance terms. This balance is expressed in ARPEGE by the summation of four components which are: the net solar radiation, the net infrared radiation, the flow of sensible heat and the flow of latent heat. Net solar radiation has been reduced to 15 Wm-2 as a spring deforestation result (Figure 4). The increase in surface albedo is the cause of this reduction. The snow layer has replaced the mask of forest vegetation. The significant decrease in net solar radiation is partially compensated by the growth of other components of the energy balance such as sensible heat flux and latent heat flux [28].

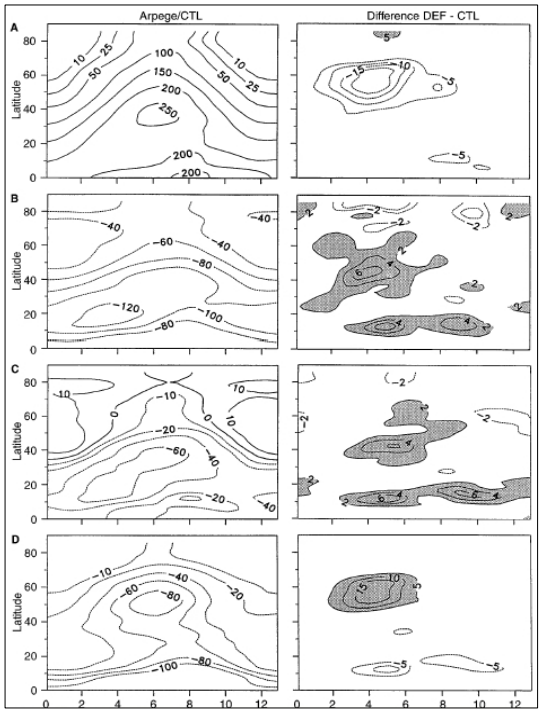

Figure 4: Seasonal cycle of Zonal mean control values (ARPEGE simulation without modification) and anomalies (deforestation scenario) of A) net solar radiation, B) net infrared radiation, C) flux of sensible heat, and D) latent heat flux in the northern hemisphere. All values are expressed in W/m2. The abscissa axis describes the months of the year, according to Douville and Royer (1997).

The latent heat flux generally decreased over the continents in response to the surface cooling phenomenon. The average value of its anomaly exceeded 15 Wm-2 in late winter and spring at mid-latitudes (Figure 4). The decrease in the latent heat flux, expressed by a positive anomaly, is explained by the following reason: the fluxes in ARPEGE are chosen to be positive when they are downward, that is, when they heat the surface. Therefore, the latent heat flux in ARPEGE is negative when there is evaporation. The decrease in evaporation will thus cause a decrease in the latent heat flux after deforestation.

The sensible heat flux decreased slightly at mid-latitudes after the deforestation scenario in ARPEGE. This decrease was about 2 Wm-2 in summer (Figure 4). The sensible heat flux represents the amount of heat exchanged by conduction between the surface and the atmosphere. The cooling of the surface in the deforestation scenario was the cause of the decrease of this flux, which may be related to the vertical diffusion generated by the turbulence over the cold continents in ARPEGE. Finally, the increase of net infrared radiation in these regions (Figure 4) was mainly due to the change in surface albedo following the change in roughness and vegetation.

Forests are very sensitive to deforestation. To better understand the interaction between forests and hydrological variability, two experiments were conducted by BOREAS in North America and NOPEX in northern Europe [8,46,47]. The experiment at the NOPEX central site in Sweden in 1995 helped explain hydrological variability in mid-latitude forests during the summer season [23]. Measurements of total precipitation, accumulated precipitation on the ground, total evaporation, transpiration and evaporation from the forest floor were used to quantify evaporation partitioning during the 1995 summer season (Table 2). Total precipitation was measured at an altitude of 100 meters. Accumulated precipitation on the ground was measured in a 5-meter x 0.1-meter aluminum insulated trough, moved to ground level. Evaporation was measured at three levels (35, 70 and 100 meters).

	Total precipitation measured (mm)	Cumulative precipitation on the ground (mm)	Total evaporation measured (mm)	Transpiration (mm)	Forest soil evaporation (mm)
16/05 - 31/10	250	176	322	243	56
16-19/07	23.4	17.6	11.2	5*	2.7*

*: Estimated values from the figures in Grelle et al. (1997).

Table 2: Hydrological measurements results in the Swedish boreal forest at the NOPEX site,, according to Grelle et al. (1997).

Transpiration was measured using the internal thermal conductivity method and the internal sensitivity of the tree temperature gradient at different diameters [48]. Evaporation from the forest floor was measured in an open mobile chamber measuring 0.6 square meters [49]. Finally, the water balance of forest vegetation was calculated by adding total precipitation, transpiration and evaporation from the forest floor, and subtracting the amount of precipitation accumulated on the ground from total evaporation. Total evaporation refers to transpiration, evaporation from the forest floor and intercepted evaporation (the difference between total precipitation and precipitation accumulated on the ground). The method for calculating this water balance was described in Grelle et al. (1997) [23].

The results of the various hydrological measurements in the Swedish forest have shown that evaporation is a significant component of the total water balance from the forest floor. During the measurement period from May 16 to October 31, 1995, the total precipitation accumulation was 250 mm, the cumulative precipitation on the ground was 176 mm and the intercepted evaporation was 74 mm, corresponding to 30% of the total precipitation. The cumulative total evaporation was 322 mm, the transpiration was 243 mm and the forest floor evaporation was 56 mm. The calculated total evaporation (the sum of intercepted evaporation, transpiration and forest floor evaporation) was more than 51 mm higher than the measured total evaporation. This difference represents the water storage capacity of the vegetation. In fact, two types of forest age were used in this experiment. Transpiration was measured in a dense forest (50 years old), while total evaporation was measured in a more mature forest (100 years old).

By eliminating the forest cover, the hydrological cycle will be affected. The albedo, evaporation and transpiration will consequently change which would modify the energy and water balance of the surface and the atmosphere. This experience showed that for forests with different ages can effects the hydrological system, such as intercepted evaporation and transpiration. These processes can regulate the air temperature, rainfall and humidity.

The results of a measurement campaign at the NOPEX site in Sweden, where the hydrological variability of a mid-latitude forest was studied during the summer season of 1995. Four-day period when heavy scattered precipitation occurred (July 16-19, 1995). During this period, the total precipitation accumulation was 23.4 mm and the precipitation on the ground was 17.6 mm. The difference between these two values (5.8 mm) represents the intercepted evaporation, which is the amount of water that

evaporates from the leaves and branches of the trees before reaching the ground. Intercepted evaporation is an important component of the forest water balance forest, as it reduces the water amount that infiltrates into the soil or runs off to streams and rivers. The total measured evaporation was 11.2 mm, which includes both intercepted evaporation and evaporation from the forest floor (the soil and litter layer). The sum of intercepted evaporation, forest floor evaporation and transpiration (the water vapor released by plants through their stomata) was 13.5 mm, almost half of which was transpiration (6.7 mm). Transpiration is another component of the forest water balance, as it regulates the temperature and humidity of the air and influences cloud formation and precipitation patterns. The water storage capacity of forest vegetation was between 1.5 mm and 3.3 mm during this rainy period, which means that some water remained in the vegetation after evaporation and transpiration processes. The water storage capacity depends on factors such as vegetation type, leaf area index, canopy structure, and rainfall intensity and duration. The data used for this text are from Grelle et al. (1997) [23].

Transpiration from forest vegetation makes a significant contribution to total evaporation. Its maximum value was 4mm/day over the entire measurement period. Forest floor evaporation showed a maximum value of 1mm/day. Transpiration, forest floor evaporation and intercepted evaporation, measured in this experiment, accounted for 65%, 15% and 20% of total evaporation respectively. The various measurements are presented in Table 2.

According to Granier et al (1990), forest soil evaporation differs from one region to another [50]. For example, soil evaporation in a Pinus pinaster forest accounts a 28% of total evaporation. In general, forest soil evaporation depends on several forest characteristics, such as density, soil water balance and vegetation type. For example, the evaporation rate is twice as high in a humid forest as in a dry forest under the same solar radiation conditions [23].

Transpiration is the water vapor released by plants through their stomata, forest floor evaporation is the water vapor that evaporates from the soil and litter layer, and intercepted evaporation is the water that evaporates from the leaves and branches of the trees before reaching the ground. These components were measured using different methods, such as internal thermal conductivity, open mobile chambers, and precipitation gauges [23]. The data from Table 2 show that transpiration was the dominant component of total evaporation, accounting for 65% of it. Forest floor evaporation and intercepted evaporation accounted for 15% and 20% of total evaporation, respectively. The components values varied with different factors, such as vegetation type, soil moisture, temperature, and precipitation. For example, transpiration was higher in dense forests than in mature forests, forest floor evaporation was higher in dry soils than in wet soils, and intercepted evaporation was higher in rainy periods than in dry periods. These components affect the water cycle by influencing the humidity and temperature of the air.

In forests, total evaporation plays a major role in water balance variability. Partial or total modification of the forest modifies greatly the soil water balance. This can influence directly intercepted evaporation, transpiration and evaporation from the forest floor. Douville and Royer (1997) reported a decrease in mean total precipitation and mean total evaporation of between 0.5 and 1 mm/day at mid-latitudes in spring, following the deforestation experiment [28]. This reduction was mainly due to the decrease in transpiration, which accounted for about 80% of total evaporation in the control experiment. Intercepted evaporation and evaporation from the forest floor also decreased slightly after deforestation. The component values varied with different factors, such as vegetation type, soil moisture, temperature, and precipitation. For example, transpiration was higher in dense forests than in grasslands, intercepted evaporation was higher in rainy periods than in dry periods, and evaporation from the forest floor was higher in wet soils than in dry soils. These components affect the water cycle by influencing the humidity and temperature of the air,

1.4 Aerosols

Aerosols are fine particles suspended in the air which can have a natural or anthropogenic source. The oceans produce large quantities of natural aerosols, such as organic sulphates, while urban or industrial activities produce anthropogenic aerosols, which vary from region to region [51]. The atmospheric concentration of aerosols has increased mainly due to human activity. Although the global radiative forcing of aerosols in the presence of GHGs delays global warming, their effects are not well known at the regional scale [52]. Reader and Boer (1998) have shown that the general effect of aerosols is to offset the global pattern of warming due to GHGs [53]. Carnel and Senior (1998) and Penner et al. (1998) reported surface cooling after including anthropogenic sulphate in their climate models (HADCM from the UK Meteorological Office and GCM from the University of Michigan in the USA, respectively [54,55].

1.4.1 Physical Effects

Aerosols can have direct and indirect effects on the radiative forcing in the atmosphere [56-58]. The direct effects are related to the scattering or absorption of radiation passing through their suspended layer

in the atmosphere, which results in either positive or negative radiative forcing. The indirect effects are mainly the changes in the radiative properties of clouds due to the increase or decrease of cloud condensation nuclei.

The direct radiative forcing of aerosols depends on the concentration, the complex refractive index and the hygroscopic properties of the particles dispersed in the atmosphere [55]. These factors influence greatly the atmosphere albedo and clouds by reducing the amount of solar radiation that passes through the aerosol layer in the atmosphere (Rosenfeld D. et al., 2014).

The IPCC (1996) estimated that anthropogenic sulfate aerosols, the dominant aerosols in the atmosphere, exert a negative mean global radiative forcing (surface cooling) of -0.4 Wm-2, with a

range of -0.2 to -0.8 Wm-2 [19]. The IPCC (2001a) specified that the mean global direct radiative forcing is estimated at -0.4 Wm-2 for sulfate, -0.2 Wm-2 for aerosols from biomass burning, -0.1 Wm-2 for organic carbon from fossil fuel, and +0.2 Wm-2 for black carbon from fossil fuel [3].

The indirect radiative forcing of aerosols is manifested through their effects on clouds. The increase in the number of cloud condensation nuclei by sulfate particles, for example, could reduce the mean size of water droplets during their formation (given the constant volume of water assumption in a cloud). According to Williams et al. (2001), a cloud containing small water droplets is characterized by a high albedo, which can reduce the solar radiation reaching the surface (Twomey effect) [56]. Thus, the presence of a high amount of sulfate aerosols in a cloud could decrease the amount of precipitation. The formation of small water droplets makes rainfall less likely, as the drops are lighter.

1.4.2 Data Analysis

The anthropogenic sulfate aerosol forcing experiment with the General Circulation Climate model (GCC), from the Hadley Centre in UK, simulated the climate by the effect of pre-industrial sulfate emissions (control scenario) and by the effect of anthropogenic sulfate emissions (1985 emissions added to natural emissions). The forcing of anthropogenic aerosols is reflected through the radiative impact of the cloud by the effect of its albedo (first indirect effect). A second indirect effect is considered through the amount of existing precipitation affecting the lifetime of the cloud [56]. Three simulations were used in this experiment. One simulation included both indirect effects (cloud albedo effect and the effect of its lifetime: BOTH), another simulation included only the cloud albedo effect (IND1), and a third simulation was characterized by the effect of cloud lifetime on climate (IND2). These three simulations were used in two scenarios (pre-industrial and modern) and for 30 years. Direct effects of sulfate aerosols were not included in this experiment. Therefore, a concentration of 345 ppm was imposed, as an effect of the standard CO2 of the year 1980. These three simulations were tested a second time but with only the atmospheric response (without taking into account the surface response) to determine the importance of the sea surface temperature (SST) and the response of the sea-ice interaction in the model. A-BOTH, A-IND1, and A-IND2 designated BOTH, IND1, and IND2 respectively in the three simulations with only the inclusion of the atmospheric response. The evolution of the mean global surface temperature with the simulation in BOTH (Table 3) showed a decrease of 1.37°C.

Expérience	ΔT (K)	ΔCF (Wm^{-2})	ΔP (%)
BOTH	-1.37	-1.69	-0.038
IND1	-1.17	-1.37	-0.032
IND2	-0.34	-0.38	-0.010
A-BOTH	-0.07	-1.62	
A-IND1	-0.06	-1.43	
A-IND2	-0.01	-0.29	

Table 3: Results of mean global variation of surface temperature (ΔT), cloud forcing (ΔCF) and precipitation (ΔP) by the effect of anthropogenic aerosols, at each MGC experiment, according to Williams et al. (2001).

The absence of surface response in the climate model exhibited a decrease in mean global temperature of 0.07°C due to the indirect effects of sulfate aerosols. This indicated the presence of a heat exchange mechanism between the surface (sea, ocean, ice, etc.) and the atmosphere, resulting in a lower surface temperature reduction under the effect of aerosol forcing. The indirect effect of cloud albedo was more pronounced than the effect of cloud lifetime (-1.17°C for IND1 and -0.34°C for IND2: Table 3). The global precipitation mean rate decreased by 0.038% in the BOTH scenario.

The indirect effects of sulfate aerosols (known as the cloud forcing response) show a high response on the radiative forcing of the cloud for short wavelengths in mid-latitudes (Figure 5). This response is equivalent to a reduction of almost -5 Wm-2, mainly due to the increase in the albedo of water droplets. The radiative forcing response of the cloud for long wavelengths is relatively weak in these regions (about -2 Wm-2: Figure 5). Thus, the reduction in the mean zonal surface temperature is about -3°C at mid-latitudes with a maximum of -3.5°C at 70°N latitude (Figure 5).

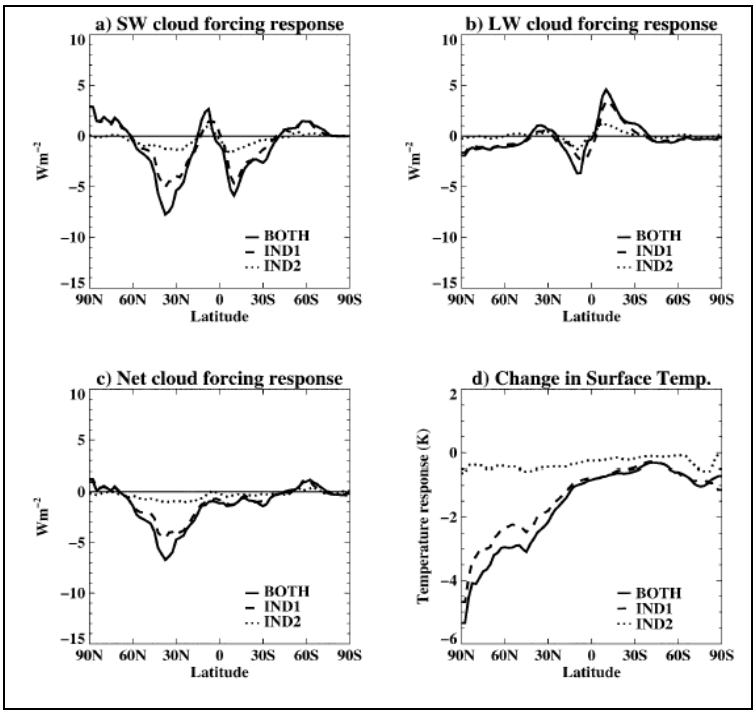

Figure 5: Evolution of the annual zonal mean of the cloud radiative forcing for a) short wavelength (SW), long wavelength (LW), net cloud radiative effect and d) surface temperature (modern – pre-industrial) of the BOTH experiment (continuous curve), IND1 and IND2, according to Williams et al. (2001).

It is difficult to quantify the direct effect of all aerosols and their evolution in time and space. The results of four climate models (Table 4) showed an increase of 1.3°C to 1.9°C by the year 2050 under the effect of GHGs and aerosols. The effect of sulfate aerosols in these models reduced global warming. The mean of this reduction was -0.5°C for the four models and -0.7°C for the CCCma. According to Boer et al. (2000), the sulfate effect was more pronounced in continental mid-latitudes, probably due to human activity in these regions [39].

	GHG +aerosols			GHG		
	1900 -present	Present -2050	2050-2100	1900-present	Present-2050	2050-2100
CCCma	0.6	1.7	2.7	0.8	2.4	3.0
GPDL	0.7	1.9		1.2	2.1	
MPI	0.5	1.5		0.8	2.1	1.7
UKMO	0.5	1.3	1.7	0.9	1.7	1.7
Mean	0.6	1.6		0.9	2.1	

Table 4: Global mean of climate sensitivity and temperature simulation (°C) following climate change, according to Boer et al. (2000).

2. Results and Discussion

Although natural factors can influence climate through solar cycles, volcanic eruptions or orbital variations, these parameters alone cannot explain the magnitude and speed of the warming observed since the last century. Since the pre-industrial period, anthropogenic factors have had a significant influence on the current climate. According to the Intergovernmental Panel on Climate Change (IPCC), it is clear that human activity is the dominant cause of the warming observed since this pre-industrial period. The IPCC bases its conclusions on scientific work and publications that analyze past and present climate data as well as future climate scenarios using climate models. One of the main evidences of human impact on the climate is the increasing concentration of greenhouse gases in the atmosphere, such as carbon dioxide (CO2), methane (CH4) or nitrous oxide (N2O). These gases capture the solar radiation part reflected by the earth's surface, which increases the temperature mean of the air and oceans. The concentration of carbon dioxide (CO2) in the atmosphere has increased by more than 40% since pre-industrial

times and reached a level not seen in at least 800,000 years. This increase is mainly due to the fossil fuels use, deforestation and land use changes. Further evidence of the impact of human activity on climate is the modification of the water cycle which will affect the distribution and intensity of precipitation, evaporation and runoff. Climate warming can cause increased of water evaporation from oceans and continents, which can increase the water vapor amount in the atmosphere. Water vapor is itself a greenhouse gas, which can in this case reinforce the GHG effect. Global warming also modifies the general circulation of the atmosphere and oceans. The latter affects its regime by affecting parameters such as humidity, pressure thus influencing precipitation and extreme atmospheric events, such as droughts, floods, storms or cyclones.

Aerosols have direct and indirect effects on radiative forcing in the atmosphere. Direct effects are linked to the dispersion or absorption of radiation passing through its layer suspended in the atmosphere which will result in a radiative forcing (positive or negative). The indirect effects are mainly variations in the radiative properties of the cloud through the growth or decay of condensation nuclei. Finally, deforestation increases surface albedo in winter, spring and early summer following the accumulation of snow in winter and the delay in its melting in spring. This variability could directly influence the physical parameters of the surface atmosphere.

To confirm our interpretations, we studied the spatial evolution of the mean surface temperature and annual precipitation during the pre-industrial period (1948-1976) and the modern period (1977-2021), using reanalysis NCEP data from the domain centered on the Mediterranean and covering Europe to the north, Asia to the east, the Atlantic Ocean to the west and North Africa to the south (20 to 55 degrees latitude and -20 to 30 degrees longitude). The annual mean processing of these data (TT and RR) showed remarkable changes after the pre-industrial period; i.e. after the year 1976.

Figure 6 shows a warming in the north of the domain, varying gradually with a latitudinal mean ranging from 0.2 °C to 0.7 °C from 25 to 35 degrees north latitude and between 0.7 °C to 0.2°C from 35 to 47 degrees north latitude. The latitude domain between 20 and 25 degrees north presents a low variability between -0.1°C and 0.1 °C. Comparing the spatial distribution of the figures 6 (a) and 6 (b), we observe a movement of thermal waves from south to north in the domain. The mean TT warming is 0.42 °C.

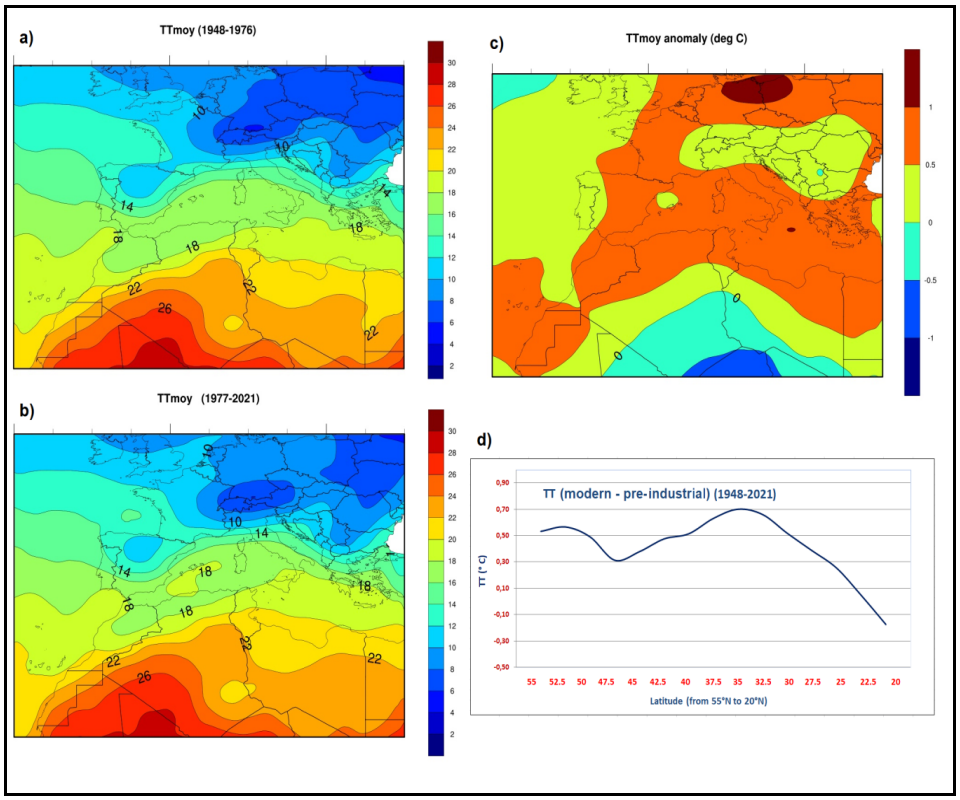

Figure 6: Spatial evolution of the surface temperature mean a) from the pre-industrial period (1948-1976), b) from the modern period (1977-2021), c) from the anomaly (modern-pre-industrial) and d) from the zonal annual mean (modern – pre-industrial).

Figure 7 shows a decrease in the annual mean precipitation in the domain, varying gradually with a latitudinal mean from 20 mm to 100 mm from 47 to 55 degrees north latitude, between 5 mm to 100 mm from 30 to 47 degrees north latitude and between 5 mm to 55 mm from 20 to 30 degrees north latitude. Comparing the spatial distribution of the figures 7 (a) and 7 (b), we observe a regional distribution weakening during the modern period, which indicates a mean decrease of 35 mm.

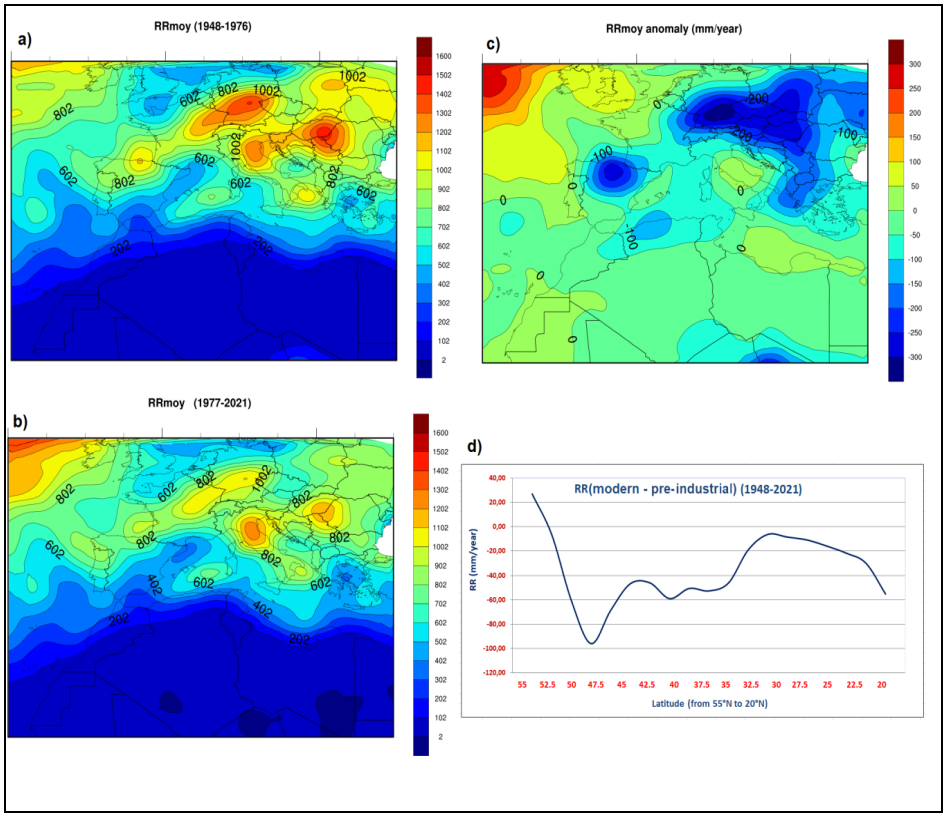

Figure 7: Spatial evolution of the annual mean precipitation a) from the pre-industrial period (1948-1976), b) from the modern period (1977-2021), c) from the anomaly (modern-pre-industrial) and d) from the zonal annual mean (modern – pre-industrial).

According to many scientific studies, the anthropogenic forcing has strengthened the concurrence of temperature over major regions in the world, particularly in the tropics, but has not yet significantly affected precipitation during the period 1948 and 2021. Indeed, global warming has apparent consequences on precipitation.

1- Conclusion

Greenhouse gases contained in the atmosphere have an important role in climate regulation. They prevent a large part of solar energy (infrared radiation) from being returned from Earth to space. Climate change is a complex context that presents a major problem that requires a multidisciplinary approach. In this paper, we have analyzed the effects of greenhouse gases (GHGs), aerosols and deforestation on the Mediterranean climate region during the 21st century, using various data sources. We have found that GHGs are the dominant factor in driving the warming of the region, while aerosols and deforestation have a modulating role, influencing the temperature and precipitation atmospheric parameters. We have discussed the uncertainties of our study, as well as the implications and challenges for the future. We hope that our paper can contribute to the scientific understanding of the Mediterranean climate and its changes, as well as to the development of effective mitigation and adaptation strategies for the region.

Funding : No funds, grants, or other support was received.

Consent for Publication: Not applicable.

Author Contributions: Daily data are collected from National Centers for Environmental Prediction (NCEP): https://crudata.uea.ac.uk/cru/data/ncep/.

Conflict of Interest: The authors declare no competing interests.

Corresponding Author: Abderrazak Arif

References

1. Ministère de la Transition Écologique. 2021. Chiffres clés du climat: France, Europe et Monde. Édition 2021. ISSN : 2557-8138,2555-7580, 92 pages.
2. Easterling, D. R., Horton, B., Jones, P. D., Peterson, T. C., Karl, T. R., Parker, D. E., ... & Folland, C. K. (1997). Maximum and minimum temperature trends for the globe. *Science, 277*(5324), 364-367.
3. Albritton, D. L., Allen, M. R., Baede, A. P. M., & Church, J. A. (2001). Summary for policymakers. A report of Working Group I of the intergovernmental panel on climate change.
4. Zhou, S., Yu, B., & Zhang, Y. (2023). Global concurrent climate extremes exacerbated by anthropogenic climate change. *Science Advances, 9*(10), eabo1638.
5. WMO. 2020. The State of Greenhouse Gases in the Atmosphere Based on Global Observations through 2019. No. 16 | 23 November 2020. SSN 2078-0796.
6. IPCC. 2014. Climate Change 2014. Synthesis Report of Intergovernmental Panel on Climate Change. 112 pages.
7. IPCC, 2023. IPCC sixth assessment report (AR6) “Climate change 2023, synthesis report of the IPCC, 36 pages.

8. Sellers, P. J., Hall, F. G., Kelly, R. D., Black, A., Baldocchi, D., Berry, J., ... & Guertin, F. E. (1997). BOREAS in 1997: Experiment overview, scientific results, and future directions. *Journal of Geophysical Research: Atmospheres, 102*(D24), 28731-28769.
9. Ressources naturelles Canada. 1999. Les changements climatiques et la forêt : Contexte du Programme scientifique du Service canadien des forêts. Service canadien des forêts. 14 pages.
10. Ressource naturelles Canada. 2000. L'état des forêts au Canada : Nos forêts au nouveau millénaire. Service canadien des forêts. 122 pages.
11. ESCWA, ACSAD, FAO, GIZ, SMHI,UN Environment, UNESCO, UNISDR, UNU-INWEH and WMO. 2017. Arab Climate Change Assessment Report. 329 pages.
12. UNESCO (United Nations Educational, Scientific and cultural Organization). 2022. World Heritage Forests, Carbon sinks under pressure. ISPN 978-92-3-100480-3, 36 pages.
13. Dale, V. H., Joyce, L. A., McNulty, S., Neilson, R. P., Ayres, M. P., & Flannigan, M. D. Hanson, PJ, Irland, LC, Lugo, AE, Peterson, CJ, Simberloff, D., Swanson. *Bioscience, 51*(9), 723-734.
14. Goody, R.M., and, Y.L., Yung, 1989. Atmospheric radiation. New York: Oxford University Press, 519 pages.
15. Harvey, L. D. (2018). *Climate and global environmental change*. Routledge.
16. Andrews, T., Gregory, J. M., Webb, M. J., & Taylor, K. E. (2012). Forcing, feedbacks and climate sensitivity in CMIP5 coupled atmosphere-ocean climate models. *Geophysical research letters, 39*(9).
17. IPCC, 2019. Special Report on the impacts of global warming of 1.5°C above pre-industrial levels and related global greenhouse gas emission pathways, in the context of strengthening the global response to the threat of climate change, sustainable development, and efforts to eradicate poverty. 630 pages.
18. IPCC. 2001b. Summary for Policymakers to Climate Change 2001: Synthesis Report of the IPCC Third assessment Report. As Approved by the XVIII Session of the IPCC at Wembley, United Kingdom, 24 to 29th September 2001. 25 pages.
19. IPCC. 1996. Climate Change 1995 - the science of climate change. In: Houghton JT, Meira Filho LG, Callander BA, Harris N, Kattenberg A., Maskell K. (eds) Contribution of Working Group I to the Second Assessment Report of the Intergovernmental Panel on Climate Change, Cambridge University Press, Cambridge, UK, p 572. IPCC. 2000. Scénarios d'émissions, Rapport Spécial du Groupe de travail III du GIEC. 19 pages.
20. Myhre, G., Shindell, D., & Pongratz, J. (2014). Anthropogenic and natural radiative forcing.
21. Wyputta, U. and B.J. McAvaney. 2001. Influence of vegetation changes during the Last Glacial Maximum using the MBRC atmospheric general circulation model. Climate Dynamics 17, 923-932.
22. Idris, O. A., Opute, P., Orimoloye, I. R., & Maboeta, M. S. (2022). Climate change in Africa and vegetation response: a bibliometric and spatially based information assessment. *Sustainability, 14*(9), 4974.
23. Grelle, A., Lundberg, A., Lindroth, A., Morén, A. S., & Cienciala, E. (1997). Evaporation components of a boreal forest: variations during the growing season. *Journal of Hydrology, 197*(1-4), 70-87.
24. Gong, T. T., Lei, H. M., Yang, D. W., Jiao, Y., & Yang, H. B. (2014). Effects of vegetation change on evapotranspiration in a semiarid shrubland of the Loess Plateau, *China. Hydrology and Earth System Sciences Discussions, 11*(12), 13571-13605.
25. Potter, G. L., Ellsaesser, H. W., MacCracken, M. C., & Ellis, J. S. (1981). Albedo change by man: test of climatic effects. *Nature, 291*(5810), 47-49.
26. Price, C., & Rind, D. (1994). The impact of a 2× CO 2 climate on lightning-caused fires. *Journal of Climate, 7*(10), 1484-1494.
27. Crowley, T. J., & Baum, S. K. (1997). Effect of vegetation on an ice-age climate model simulation. *Journal of Geophysical Research: Atmospheres, 102*(D14), 16463-16480.
28. Douville, H., & Royer, J. F. (1996). Influence of the temperate and boreal forests on the Northern Hemisphere climate in the Météo-France climate model. *Climate Dynamics, 13*(1), 57-74.
29. Xue, Y., Liou, K. N., & Kasahara, A. (1990). Investigation of biogeophysical feedback on the African climate using a two-dimensional model. *Journal of Climate, 3*(3), 337-352.
30. Rind, D. (1984). The influence of vegetation on the hydrologic cycle in a global climate model. *Climate Processes and Climate Sensitivity, 29*, 73-91.
31. Levine, J. S. (Ed.). (1991). *Global biomass burning: atmospheric, climatic, and biospheric implications*. MIT press.
32. Li, C. and C. Lai. 1991. A study of climate change related to deforestation in the Xishuangbanna area. Yunnam, Clim. Global Biomass Burning, J. Levine, Ed., The MIT Press, 477-482. .
33. Zhang, X., Jiao, Z., Zhao, C., Qu, Y., Liu, Q., Zhang, H., ... & Cui, L. (2022). Review of land surface albedo: Variance characteristics, climate effect and management strategy. *Remote Sensing, 14*(6), 1382.
34. Buttar, N. A., Hu, Y., Tanny, J., Raza, A., Niaz, Y., Khan, M. I., ... & Bilal Idrees, M. (2022). Estimation of Sensible and Latent Heat Fluxes Using Flux Variance Method under Unstable Conditions: A Case Study of Tea Plants. *Atmosphere, 13*(10), 1545.
35. Anthes, R.A. 1997. Meteorology, seventh Edition. The University Corporation for Atmospheric Research Boulder, Colorado. Upper Saddle River, New Jersey 07458. 214 pages.
36. Hartmann. D.L. 1994. Global Physical Climatology. Department of Atmospheric Sciences, University of Washington, Seattle, Washington, Academic Press, 411 pages.
37. Manabe, S., & Wetherald, R. T. (1987). Large-scale changes of soil wetness induced by an increase in atmospheric carbon dioxide. *Journal of the Atmospheric Sciences, 44*(8),

1211-1236.
38. Laprise, R., Caya, D., Giguere, M., Bergeron, G., Côté, H., Blanchet, J. P., ... & McFarlane, N. A. (1998). Climate and climate change in western Canada as simulated by the Canadian Regional Climate Model. *Atmosphere-Ocean, 36*(2), 119-167.
39. Boer, G. J., Flato, G., & Ramsden, D. (2000). A transient climate change simulation with greenhouse gas and aerosol forcing: projected climate to the twenty-first century. *Climate dynamics, 16*(6), 427-450.
40. Flato, G. M., Boer, G. J., Lee, W. G., McFarlane, N. A., Ramsden, D., Reader, M. C., & Weaver, A. J. (2000). The Canadian Centre for Climate Modelling and Analysis global coupled model and its climate. *Climate Dynamics, 16*(6), 451-467.
41. Richardson, M. T. (2023). A Physical Explanation for Ocean Air–Water Warming Differences under CO 2-Forced Warming. *Journal of Climate, 36*(9), 2857-2871.
42. Harvey, L. D. (1988). On the role of high latitude ice, snow, and vegetation feedbacks in the climatic response to external forcing changes. *Climatic Change, 13*(2), 191-224.
43. Chalita, S., & Le Treut, H. (1994). The albedo of temperate and boreal forest and the Northern Hemisphere climate: a sensitivity experiment using the LMD GCM. *Climate Dynamics, 10,* 231-240.
44. Thomas, G., & Rowntree, P. R. (1992). The boreal forests and climate. *Quarterly Journal of the Royal Meteorological Society, 118*(505), 469-497.
45. Déqué, M., Dreveton, C., Braun, A., & Cariolle, D. (1994). The ARPEGE/IFS atmosphere model: a contribution to the French community climate modelling. *Climate Dynamics, 10*, 249-266.
46. Sellers, P.J., Hall, F.G., Ranson, J., Margolis, H., Kelly, B., Den Hartog, J., Vhilar, J., Ryan, M., Goodison, B., Crill, P., Lettenmair, D. and Wickland, D.E. 1995. The boreal ecosystem atmosphere study (BOREAS). Ann. Geophys. Suppl. 11, 13(2), C524 (abstr.).
47. Halldin, S., Gottschalk, L. Van de Griend, A.A., Gryning, S.-E., Heikinheimo, M., Hogstrom, V., Jochum, A., and Lundin, L.-C. 1995. Science plan for NOPEX. Technical Report N°12, Upsala University, Upsala, 38 pages.
48. Čermák, J., Cienciala, E., Kučera, J., Lindroth, A., & Bednářová, E. (1995). Individual variation of sap-flow rate in large pine and spruce trees and stand transpiration: a pilot study at the central NOPEX site. *Journal of Hydrology, 168*(1-4), 17-27.
49. Iritz, Z., Lindroth, A., & Gärdenäs, A. (1997). Open ventilated chamber system for measurements of H2O and CO2 fluxes from the soil surface. *Soil Technology, 10*(3), 169-184.
50. Granier, A., Bobay, V., Gash, J. H. C., Gelpe, J., Saugier, B., & Shuttleworth, W. J. (1990). Vapour flux density and transpiration rate comparisons in a stand of Maritime pine (Pinus pinaster Ait.) in Les Landes forest. *Agricultural and Forest Meteorology, 51*(3-4), 309-319.
51. Renoux, A., & Boulaud, D. (1998). Les aérosols: physique et métrologie. Tec & Doc Lavoisier.
52. Hengeveld, H. 1995. Understanding Atmospheric Change. Second Edition. Atmospheric environment service. Environnement Canada. Report N 95-2, 71 pages.
53. Reader, M. C., & Boer, G. J. (1998). The modification of greenhouse gas warming by the direct effect of sulphate aerosols. *Climate Dynamics, 14,* 593-607.
54. Carnell, R. E., & Senior, C. A. (1998). Changes in mid-latitude variability due to increasing greenhouse gases and sulphate aerosols. *Climate Dynamics, 14,* 369-383.
55. Penner, J. E., Chuang, C. C., & Grant, K. (1998). Climate forcing by carbonaceous and sulfate aerosols. *Climate Dynamics, 14*, 839-851.
56. Williams, K. D., Jones, A., Roberts, D. L., Senior, C. A., & Woodage, M. J. (2001). The response of the climate system to the indirect effects of anthropogenic sulfate aerosol. *Climate Dynamics, 17*, 845-856.
57. Sekiguchi, M., Nakajima, T., Suzuki, K., Kawamoto, K., Higurashi, A., Rosenfeld, D., ... & Mukai, S. (2003). A study of the direct and indirect effects of aerosols using global satellite data sets of aerosol and cloud parameters. *Journal of Geophysical Research: Atmospheres, 108*(D22).
58. Salah, Z., Shalaby, A., Steiner, A. L., Zakey, A. S., Gautam, R., & Abdel Wahab, M. M. (2018). Study of aerosol direct and indirect effects and auto-conversion processes over the West African monsoon region using a regional climate model. *Advances in Atmospheric Sciences, 35*, 182-194.
59. Environnement Canada. 1997. Impacts et adaptation à la variabilité et au changement du climat. Tome V de l'étude pan-canadienne : Impacts et adaptation au climat. 266 pages.
60. Environnement Canada. 1999. Vulnérabilité et adaptation aux changements climatiques. 114p.
61. IPCC. 2013 . Climate Change 2013: The Physical Science Basis. Contribution of Working Group I to the Fifth Assessment Report of the Intergovernmental Panel on Climate Change [Stocker T.F., Qin D., Plattner G.-K., Tignor M., Allen S.K., Boschung J., Nauels A., Xia Y., Bex V., Midgley P.M.(eds.)]. Cambridge University Press.
62. Rosenfeld, D., Sherwood, S., Wood, R., & Donner, L. (2014). Climate effects of aerosol-cloud interactions. *Science, 343*(6169), 379-380.
63. Otterman, J., Chou, M. D., & Arking, A. (1984). Effects of nontropical forest cover on climate. *Journal of Applied Meteorology and Climatology, 23*(5), 762-767.